Restoring Force Characteristics of the Steel Frames of Nuclear Power Station Buildings
(Part 1) - Setting up Restoring Force Characteristics Models -

N. NAKAMURA
The Tokyo Electric Power Company Inc., Tokyo, Japan
H. TOMURA, Y. TAKAHASHI
Obayashi Corporation, Tokyo, Japan
T. SAEKI, N. TANAKA
Kajima Corporation, Tokyo, Japan
Y. INADA, T. HIROTANI
Shimizu, Corporation, Tokyo, Japan

1. INTRODUCTION

In order to design nuclear power station buildings estimating quantitatively seismic safety of the buildings during large scale earthquakes, it is effective to perform dynamic nonlinear seismic response analysis using reasonable restoring force characteristics. A means of evaluating the restoring force characteristics of the reinforced concrete structures of most nuclear reactor buildings has already been proposed, and if the restoring force characteristics of the steel framed buildings such as the turbine building are set up, it is possible to calculate the overall behavior of the buildings during large scale earthquakes.

Steel structures are designed so that resistance to the earthquake load is taken up in the X and K type braces. Consequently, it is necessary to investigate and formulate the elasto-plastic behavior of these braces to evaluate the restoring force characteristics of the steel frames.

In this paper, by using data obtained in experiments on reduced scale specimens of actual size of X type braces and by analyzing data previously obtained from K type brace experiments, we will propose simple and practical restoring force characteristics models of both types of the braces in the steel framed buildings.

2. THE STATUS QUO OF STEEL FRAMES

The major factors affecting the restoring force characteristics of braces are their shapes, slenderness ratio, width-to-thickness ratio, their kinds of joint types and so on. The research results on actual nuclear power station buildings are shown in Table 1.

3. THE RESTORING FORCE CHARACTERISTICS OF X TYPE BRACES

3.1 Outline of the model tests (Kato, B. et al. 1990)

1) Specimens and loading method

Experiments were conducted within the parameters of: slenderness ratio (40, 60, 80), flange width-to-thickness ratio (6, 9, 13) and joint types (B, C, D), to investigate elasto-plastic hysteresis characteristics of X type braces. The experiments were performed on 11 reduced scale (1/2.5 or 1/3.5) models simulating standard frame dimensions and details as in Table 1. The combination of the parameters and the meaning of the specimen names are shown in Table 2. A typical configuration of a specimen is shown in Fig. 1. SS41 was the material used for the braces and material properties are shown in Table 3. The joints were made using high strength bolted connections in friction type.

SMiRT 11 Transactions Vol. K (August 1991) Tokyo, Japan, © 1991

The test specimen was fixed to the test bed, and cyclic lateral load equivalent to an earthquake was applied to both left and right ends of the beam.

2) Test results
The relationships between the shearing force shared by the braces and the shearing deformation angle were computed from the deformations and strains at measuring points, and are shown in Fig. 2 (as the $q-\gamma$ curve). q is the shear force normalized by the yielding axial force of the brace, and γ is the shearing deformation angle normalized by the height of the specimen.

3) The $q-\gamma$ curve
The important conclusions which can be drawn from the $q-\gamma$ curve are as follows:

- The restraining effect of the joints based on the deformation mode of the brace after buckling can be evaluated as the effective buckling length αL (α: Coefficient of the buckling length), which is $\alpha = 0.65$ in bracket and composite gusset plate types, and $\alpha = 0.40$ in double gusset plate types. In each type, the restraining effect is quite high.
- The maximum strength of the brace can be approximated by the sum of the buckling strength with α and the yielding axial force.
- If the effective buckling length and the effective slenderness ratio ($\overline{\lambda_e}$) are introduced, it becomes easier to judge the merits and demerits of the hysteresis characteristics. The $\overline{\lambda_e}$ values for each specimen are shown in Fig. 2.

$$\overline{\lambda_e} = \alpha\ (L / i_y)\ \sqrt{F / (\pi^2 E)}$$

where, E : Modulus of elasticity
F : Basic value used in determining allowable stresses

- The $q-\gamma$ relationship has degrading bi-linear or tri-linear skeleton curve. The hysteresis characteristics depend upon $\overline{\lambda_e}$ and the width-to-thickness ratio: where $\overline{\lambda_e}$ is small, the characteristics show stable spindle shape, and where $\overline{\lambda_e}$ is large, those show the combination of the perfect elasto-plastic type and the pinching type. The hysteresis characteristics of the specimen having larger $\overline{\lambda_e}$ show the tendency that the pinching occurs at the smaller deformation and at the lower load. Also the higher the width-to-thickness ratio, the earlier local buckling occurs and the larger the strength deterioration.
- The types of brace failure can be categorized into breakage at the part with local backling, breakage at welded part of joint, and breakage at connecting portion having a loss of the section area, but in every type this occurs when γ is above 2/100.

3.2 Setting up restoring force characteristics

Considering the test results and the practicality for the design and based on:
① the bi-linear skeleton curve;
② hysteresis characteristics comprising of the perfect elasto-plastic type and pinching type;
③ $\overline{\lambda_e}$ determines the shape of the skeleton curve and the proportion of the perfect elasto-plastic type to the vertex strength;
the restoring force characteristics of X type braces can be set up. This can be explained by the flow as in Fig. 4.

1) Skeleton curve
From the envelopes of the $q-\gamma$ curves obtained from the tests, the energy equivalent strength (q_B') shown in Fig. 3 may be applied to give the vertex strength(Q_1) in the bi-linear skeleton curve.

$$Q_1 = 2N_Y \cos\theta / (0.710 + 1.12\overline{\lambda_e}),\quad \gamma_1 = Q_1 / K_1$$

where, N_Y, K_1: Yielding axial force of brace, Initial shear stiffness
θ : Angle formed by brace and beam in braced frame

2) Hysteresis characteristics
Using the reference (Kato,B. et al. 1977), the above skeleton can be divided into the skeleton curves of the perfect elasto-plastic type and the pinching

type. As in Fig. 4, the distribution ratio(β_1) can be used to calculate the vertex strength and the stiffness in each type.

$$\beta_1 = 1.29 - 1.12\,\overline{\lambda_e}$$

3) Setting up restoring force characteristics
By superposing the skeleton curves of the perfect elasto-plastic type and the pinching type, the restoring force chracteristics of X type braces can be obtained. Fig. 5 shows the comparison with the test results and the proposed restoring force characteristics.

4. THE RESTORING FORCE CHARACTERISTICS OF K TYPE BRACES

4.1 Past research results

The restoring force characteristics of K type braces in Table 1 can be evaluated by past studies (Kato,B. et al. 1983, Muto,K. et al. 1985).
The trend in the relationships between the horizontal load (Q) and the horizontal deformation (δ) may be observed as a result.

- The influence of joint type on the relationships is almost the same as for X type braces.
- The $Q-\delta$ relationship depends upon $\overline{\lambda_e}$ and the strength and the stiffness of the beams and outer rigid frame.
- If the strength of the beam is sufficiently greater than that of the braces, the restoring force characteristics can be evaluated by the method for X type braces.
- A representative case of the $Q-\delta$ relationship where the beam is weak in comparison with the braces may be found in Fig. 6. There is no sign of pinching and quite stable characteristics are displayed. The restoring force characteristics are assumed to be a combination of the perfect elasto-plastic type and the peak-oriented type.

4.2 Setting up restoring force characteristics

Considering the past studies and the practicality for the design and based on:
① setting up the restoring force characteristics of the rigid frame with braces;
② the bi-linear skeleton curve;
③ hysteresis characteristics comprising of the perfect elasto-plastic type and the peak-oriented type;
④ the shape of the skeleton curve and the propotion of the perfect elasto-plastic type to the vertex strength are determined by the characteristics of both the braces and the rigid frame;
the restoring force characteristics in the case of weak beam can be set up. This can be explained by the flow as in Fig. 7.

1) Skeleton curve
The vertex strength (Q_1) should be the sum of the strength of the rigid frame (Q_R), the strength of the tensile brace (Q_T) and the strength of the compressive brace (Q_c) (Kato,B. et al. 1983).

$$Q_1 = Q_R + Q_T + Q_c,\quad \gamma_1 = Q_1 / K_1$$

where, K_1: Stiffness of rigid frame with braces

2) Hysteresis characteristics
The above skeleton curve can be divided into the skeleton curves of the perfect elasto-plastic type and the peak-oriented type. As in Fig. 7, the distribution ratio(β_2) obtained from the coefficient(C) can be used to calculate the vertex strength and the stiffness in each type.

$$\beta_2 = 0, \qquad \text{(provided that } C \leqq 0.76\text{)}$$
$$\beta_2 = 0.15\ (C-0.76),\ 0 \leqq \beta_2 \leqq 1.0, \qquad \text{(provided that } C > 0.76\text{)}$$

where, $C = (1/\overline{\lambda_e}^2)\cdot(K_R/K_1)\cdot(N_Y\cdot H\cdot\cos\theta/{}_bM_P)$,
K_R: Initial stiffness of rigid frame only, H: Height of story,
N_Y: Yielding axial force of brace, ${}_bM_P$: Beam's fully plastic moment

3) Setting up restoring force characteristics
By superposing the skeleton curves of the perfect elasto-plastic type and the peak-oriented type, the restoring force characteristics of K type braces can be obtained. Fig. 6 shows the comparison with the past research results and the proposed restoring force characteristics.

5. CONCLUSION

X and K type braces are the principal earthquake resistant elements in the steel frames of nuclear power station buildings. Therefore the results of past reseach and experiments were examined, and 11 reduced scale models simulating actual X type braced frames were subjected to static lateral loading tests. The simple and practical restoring force characteristics models were proposed for the design of the X and K type braces.

This study was carried out as a part of joint research study by ten electric power companies in Japan (Tokyo, Hokkaido, Tohoku, Chubu, Hokuriku, Kansai, Chugoku, Shikoku, Kyushu and Japan Atomic) being cooperated by five construction companies (Obayashi, Kajima, Shimizu, Taisei and Takenaka). This work was performed by the guidance of "Committee of Research" chaired by Prof. Ben Kato (The University of Tokyo). The authors wish to acknowledge to the valuable cooperation and suggestions given by the members of the Committee.

REFERENCES

Kato,B., Nakamura,N. et al. (1990). Study on Restoring Force Characteristics of Steel Frames in Buildings of Nuclear Power Stations, Part 1～Part 7, Structure II, Summaries of Technical Papers of Annual Meeting, A.I.J., pp.1531-1544

Kato,B. and Akiyama,H. (1977). Restoring Force Characteristics of Steel Frames Equipped with Diagonal Bracings, Transactions of A.I.J., pp.99-107

Kato,B. and Mukai,A. (1983). Strength and Ductility of K-type Braced Frame, A.I.J., (Kanto Chapter Research Report), pp.277-280

Muto,K. et al. (1985). A Demonstrative Study of Aseismic Design on a Large Turbine Building with K-Braced Frame, Transactions of A.I.J., pp.66-76

Table 1 Tendencies of X– and K–braced frames

			X Braced Frame			K Braced Frame		
Rigid Frame	Dimensions		Average S : H = 1 : 1 S = H = 7.0m L = 5.0m 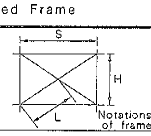			Average S : H = 1 : 0.5 S = 9.6m H = 4.5m L = 6.6m 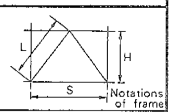		
	Steel Variety		SM50 (PWR type) SS41 (BWR type)			Same as that of X Braced Frame		
Brace			Minimum	Mean	Maximum	Minimum	Mean	Maximum
	Slenderness ratio		35	60	90	39	78	117
	Width – to – thickness ratio	Flange	4	8.5	14.5	5.2	9.4	13.4
		Web	12	25	40	14.3	23.8	27.5
	Joint Type		B		C		D	
			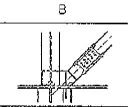		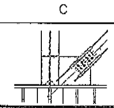		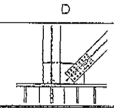	

Joint Type
- B Type — Bracket Type ··················· In Plane Strong Axis
- C Type — Composite Gusset Plate Type ···· In Plane Strong Axis
- D Type — Double Gusset Plate Type ······· Out – of – plane Strong Axis

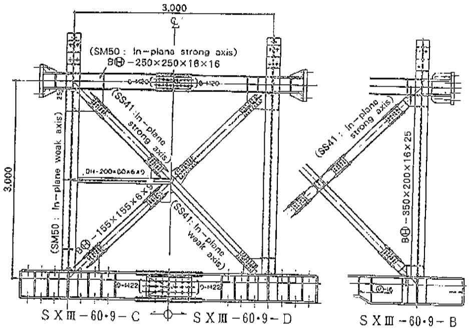

Fig.1 Configuration of specimens

Table 2 List of specimens

Brace Member			Joint Type			Dimensions of Rigid Frame
λ	$\frac{b}{t_f}$	Section Size	Bracket Type (B Type)	Composite Gusset Plate Pype (C Type)	Double Gusset Plate Type (D Type)	
40	6.0	H − 155 × 155 × 6 × 12 (35 *1 , 6.5 *2)	SX Ⅱ − 40 · 6 − B *3	——	——	S = H = 2.0m
	9.0	H − 155 × 155 × 6 × 9 (36 , 8.6)	SX Ⅱ − 40 · 9 − B	——	——	
60	6.0	H − 155 × 155 × 6 × 12 (52 , 6.5)	SX Ⅲ − 60 · 6 − B	——	——	S = H = 3.0m
	9.0	H − 155 × 155 × 6 × 9 (55 , 8.6)	SX Ⅲ − 60 · 9 − B	SX Ⅲ − 60 · 9 − C	SX Ⅲ − 60 · 9 − D	
	13.0	H − 155 × 155 × 6 × 6 (57 , 12.9)	SX Ⅲ − 60 · 13 − B	——	——	
80	9.0	H − 110 × 110 × 6 × 6 (80 , 9.4)	SX Ⅲ − 80 · 9 − B	SX Ⅲ − 80 · 9 − C	——	
Remarks			Rigid Frame Specimen SO Ⅱ : S = H = 2.00m SO Ⅲ : S = H = 3.00m			

*1 : Actual slenderness ratio

*2 : Actual width − to − thickness ratio

*3 : Meaning of Specimen Name

Ex.) S X Ⅱ − 40 · 6 − B

- Joint type
- Flange width − to − thickness ratio of brace (b/t_f)
- Slenderness ratio of brace (λ)
- Dimensions of rigid frame
  - Ⅲ : 3.0m (height of story and span)
  - Ⅱ : 2.0m (height of story and span)
- Existence of brace
  - X : Specimen with X type brace
  - O : Specimen without brace
- S signifies steel construction

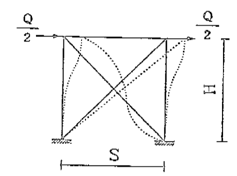

Table 3 Material properties

Test piece	Upper yield point σ_y (tonf/cm²)	Tensile strength σ_u (tonf/cm²)	$\frac{\sigma_y}{\sigma_u}$	Rapture strain (%)
PL−6	3.77	4.98	0.757	22.4
PL−9	2.88	4.41	0.654	29.0
PL−12	2.70	4.32	0.626	31.2

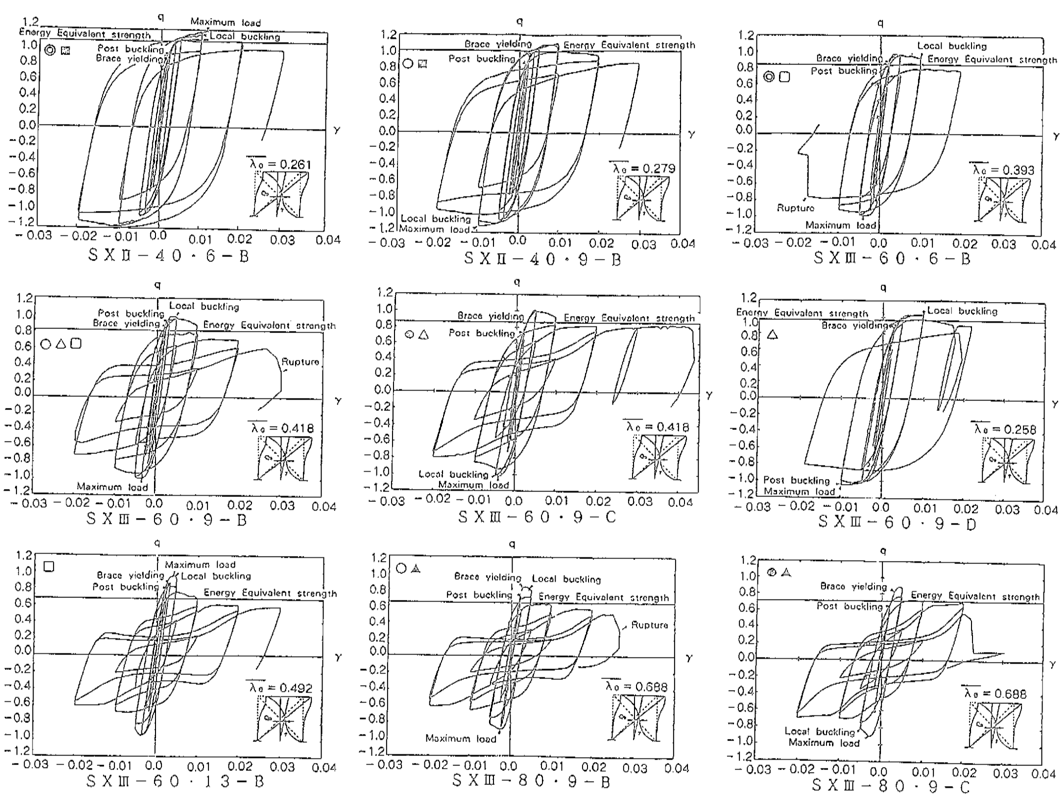

○ Series comparison of slenderness ratio
△ Series comparison by joints types
□ Series comparison of width−to−thickness ratio

Fig.2 Normalized load−deflection curves (q− γ relationship)

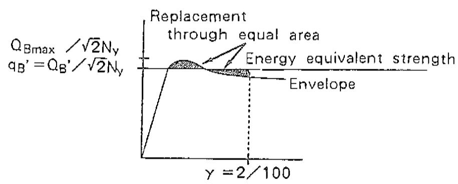

Fig.3 Replacement with bi−linear type through energy equalization

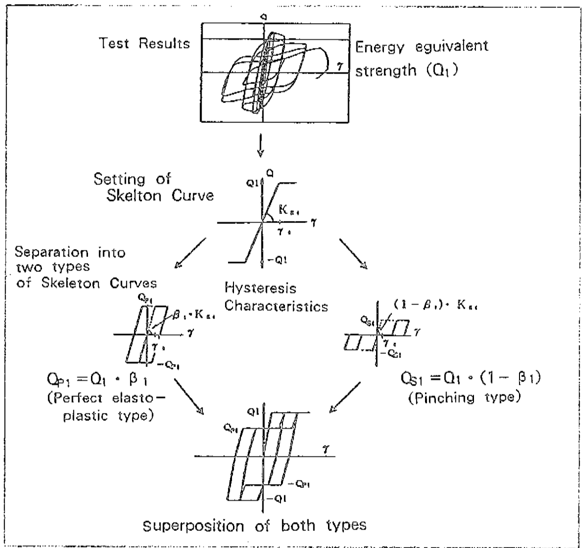

Fig.4 Flow chart for setting up restoring force characteristics for the design of X type brace (Proposed method for X type brace)

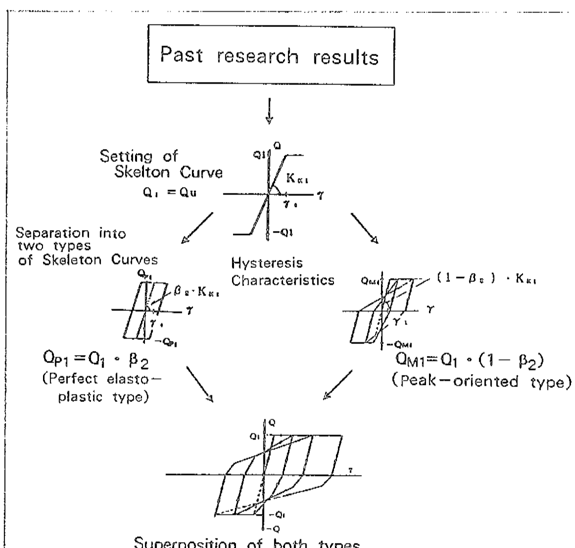

Fig.7 Flow chart for setting up restoring force characteristics for the design of K type brace (Proposed method for K type brace)

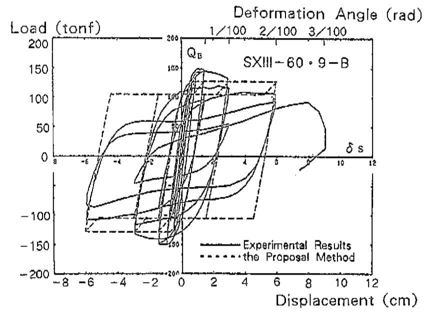

Fig.5 Comparison with test results and proposed method for X type brace

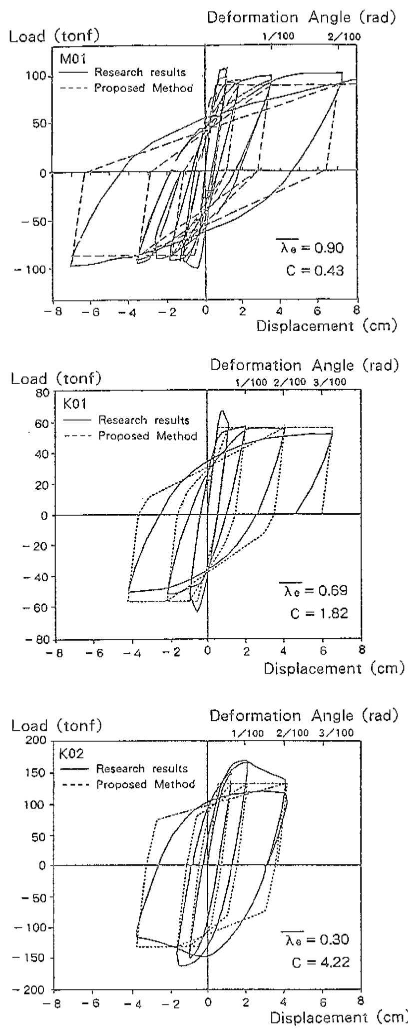

Fig.6 Comparison with past research results and proposed method for K type brace